Research on a Novel Switched Reluctance Wind Power Generator System for Electric Vehicles

Y.J. BAO[1]   K.W.E. CHENG[2]   B.P. DIVAKAR[3]

[1] Department of Electrical Engineering, The Hong Kong Polytechnic University, Hong Kong
E-mail: eeyjbao@polyu.edu.hk
[2] Department of Electrical Engineering, The Hong Kong Polytechnic University, Hong Kong
E-mail: eeecheng@polyu.edu.hk
[3] Department of Electrical Engineering, The Hong Kong Polytechnic University, Hong Kong
E-mail: eediva@polyu.edu.hk

Abstract–The exigencies created by the shortage of energy supplies and the ever-growing air pollution stress the need for an alternative solution to the on-board power generation. The purpose of this paper is to develop a novel switched reluctance wind power generator (SRWPG) system for electric vehicles (EVs), which can convert the wind power into electric power so as to charge a battery or support other vital loads in an EV on-board. The work will focus on collecting valuable first hand experience in the wind assisted on-board power generation system. Various configurations of the wind turbines are studied and the one suitable to the project is proposed in the investigation. In addition to the mechanical aspect of the SRWPG system due attention is given to the control aspect of the system according to the characteristics of switched reluctance generators (SRGs).

Keywords–Wind power, wind turbines, switched reluctance generators (SRGs), switched reluctance wind power generators (SRWPGs), electric vehicles (EVs).

I. INTRODUCTION

Automobiles that run on fossil based fuels are considered as one among the major contributors to air pollution although the present engines are much superior to their earlier counterparts. Many solutions for minimizing pollution and to minimize the dependency on the fossil based fuel have been suggested. Accordingly electric vehicles (EVs) and hybrid electric vehicles (HEVs) show very encouraging results in cutting down the pollution [1], [2]. Pure EVs use batteries as energy sources which must be fully charged overnight to ensure the vehicle can be used for the designated mileage before recharging is required. The use of the battery coupled with the short of charging infrastructure and long charging time are some of the reasons for the slow acceptance of pure EVs in the market. So, other alternative sources such as solar, fuel cells and wind have been used in conjunction with the primary battery source. The advantage of the alternative solutions is that the power can be generated on board even when the vehicle is stationary thus permitting the usage of luxury loads such as air conditioning (AC) and music without the risk of air pollution. This is in contrast to the vehicles with gasoline engine which must be idling to support loads when the vehicle is at rest. The concept of on-board power generation to drive certain loads when the engine is switched may become an integral part of any vehicular electrical design in the future due to environmental issues. The ever increasing demand for power from passenger's comforts loads and the possible ban or penalty against idling engines may encourage the use of other alternative sources for on-board power generation. The other advantage of on-board power

generation using alternative sources is that the batteries can be charged while the vehicle is in motion thus reducing the reliance on the charging station and improving the driving mileage from the batteries.

Fuel-cells based on-board power generation is proposed in [3]. The dual voltages, 42/14 V, proposed in the paper are used for driving the air conditioner and charging the battery respectively. The cost of the Fuel cells, storage and life cycle are the challenges yet to be addressed for commercial application. The application of photovoltaic (PV) cells has been discussed in [4], but solar based on-board power generation is too bulky for automotive application [1]. Since the technology of wind power generation has matured rapidly, wind power, as an alternative zero-emission energy source, has attracted interest from government organizations and automotive industries. The concept of harnessing wind power by mounting number of small wind capturing units on a vehicle is discussed in [5] and [6].

The switched reluctance machine owing to its simple robust structure, its inherent temperature insensitive property due to the absence of field coils, and fault tolerance ability makes one of the ideal choices for wind power generation. The ability to maintain high efficiency at different speeds and the capability to operate under harsh automotive environment are the other reasons for the growing interest in the use of switched reluctance machine for wind power generation. The use of switched reluctance machine for wind power generation has been discussed in [8], [12], [13].

The main objectives of the present investigation are to build a wind power assisted switched reluctance generators (SRGs) to charge batteries and to support other vital loads in an EV. The study will focus on the practical issues in the design of an integrated system that is suitable for an EV. The paper is organized as follows: the novel EV with the SRWPG system is pointed out in II, selection of the mounting location of the integrated system is discussed in III, the operating principle and the model of SRGs are discussed in IV, the proposed switched reluctance wind power generator (SRWPG) system is discussed in V following by concluding remarks in VI.

II. THE STRUCTURE OF THE NOVEL EV

Normally, wind power generation is associated with the traditional stationary wind turbine structures erected on ground. However, the current investigation is focused on

capturing the wind force on a moving vehicle for generating electrical power on-board. It is envisaged that the proposed method will enhance the driving distance available from the traditional electric vehicles and make the use of EVs very attractive for long journeys.

Pure EVs are one of the solutions proposed to tackle the energy crisis and global warming. However, short driving range, long charging time have proved the limitation of pure EVs. The HEV was developed to overcome these disadvantages of the pure EV. But its development is influenced by its inherent disadvantages, such as the high cost, the complex energy management system and the emission from the internal combustion engine (ICE).

Based on the above discussion, a novel wind power hybrid EV is proposed here. The architecture of the wind power hybrid electric vehicle is shown in Fig. 1, and is line with the dual voltage series HEV architecture [2] that is being popularly touted as one of the solutions for the ever-increasing in-vehicle load demand. In the novel EV, the wind power is first converted into electricity using a switched reluctance generator and the energy generated is used to charge the battery or can be used to support the propulsion system and other loads of EVs, such as AC, power steering, lighting system, and so on.

Conceptually, it is a wind-assisted EV that aims to extend the driving range comparable with that of conventional vehicle. The wind-assisted EV poses number of challenges which must be addressed for successful implementation. Therefore the present investigation aims at acquiring first hand experience for the practical implementation of such an SRWPG system for on-board power generation.
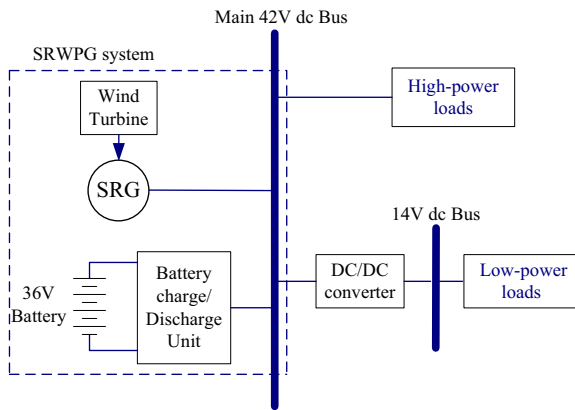

Fig. 1: Schematic of a dual voltage series hybrid architecture using one battery

III. MOUNTING LOCATIONS AND WIND TURBINE STRUCTURE

The mounting location and the structure of wind turbine for on-board power generation have to satisfy several factors for successful integration of the turbine and the switched reluctance generator. Following factors have to be addressed for such an application:
a. The system should not cause appreciable drag;
b. Should not block the driver's view;
c. Should capture as much wind power as possible;
d. Should not hamper the aesthetic appeal of the vehicle.

1. The fixed locations of the wind turbines

The mounting of the wind turbine integrated SRG is a real challenge in the EV application. The mounting location of the wind turbine is very crucial for the operation unlike the case with fuel-cells. The mounting location also depends on the structure of the wind turbine. For example, a wind turbine with large blades cannot be mounted on top or front of the vehicle and must be mounted only at the back. On the other hand a wind turbine with drum like rotating blades cannot be mounted where it is not exposed to wind flow. The other issue to be considered for the mounting location is the way the turbine is coupled to the generator. In view of the complexity involved in the mechanical fixture of the unit the front hood of a vehicle is chosen as the mounting location for the unit chosen in the current work. The structure of the wind turbine selected for this work is discussed next.

2. The structure of the wind turbines

The regular wind turbines with fewer blades cannot be mounted because of the large wind span of the blades. On the other hand, if the wind span of the blades is reduced the turbine cannot capture enough wind power. Another option is to use number of smaller wind turbines mounted at various locations to generate the required electrical power but this option requires as many generators as the number of turbines. In order to overcome the limitations a wind turbine as in Fig. 2a is considered for the proposed integration. The advantage of this preferred structure is the easy coupling of the generator with two coaxially mounted wind turbines as shown in Fig. 2b.
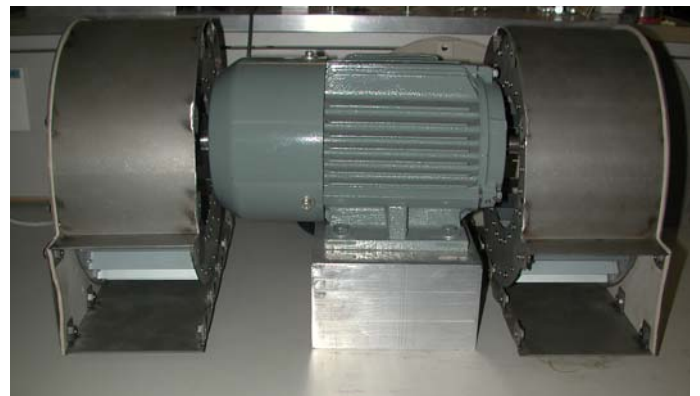

Fig. 2 (a): Wind turbine

Fig. 2 (b): Integrated wind turbine

3. The model and the characteristics of the wind turbine

3.1 The model of the wind turbine

The mechanical torque produced by a wind turbine is [12]

$$T_m = \frac{1}{2}\pi\rho C_t(\lambda,\beta)R^3V^2 \tag{1}$$

where $C_t(\lambda,\beta)$ is the torque coefficient, ρ is the air density, R is the blade radius, β is the blade pitch angle, V is the wind velocity, and λ is the tip-speed ratio defined as

$$\lambda = \frac{\omega_T R}{V} \tag{2}$$

where ω_T is the rotational speed of the blades. The power captured from the wind turbine is obtained as

$$P_m = \frac{1}{2}\pi\rho C_p(\lambda,\beta)R^2V^3 \tag{3}$$

$$C_p(\lambda,\beta) = \lambda C_T(\lambda,\beta) \tag{4}$$

where $C_p(\lambda,\beta)$ is the power coefficient.

3.2 The characteristics of the variable-speed wind turbine

The power output from a wind turbine is not uniform and depends on wind speed (3) as shown in Fig. 3. The maximum power output depends on $C_p(\lambda,\beta)$ which can be controlled in a variable speed wind turbine. For high speed, when wind turbine speed $n > n_c$, the output power reaches the maximum power of the wind turbine system. In this case, the output power is equal to the maximum power all the time and wind turbines cannot operate at the maximum $C_p(\lambda,\beta)$. As a result, the wind power generator should be avoided to work in this region.
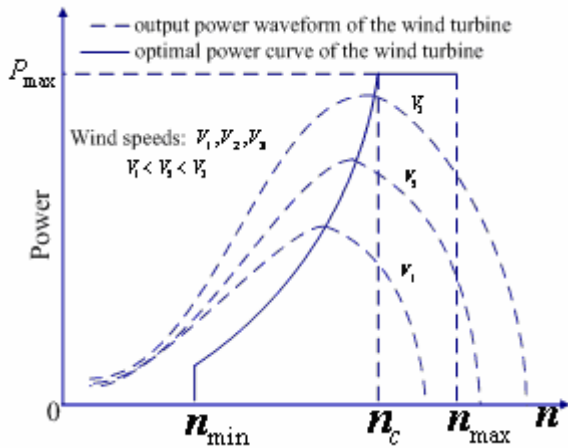

Fig. 3: The power-speed characteristics of the wind power
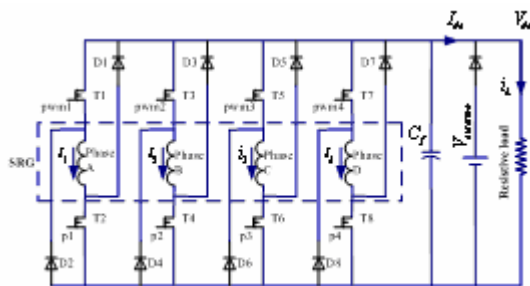
IV. THE MODEL AND THE CHARACTERISTICS OF SRGS

Fig. 4: The structure of the power converter

1. The model of SRGs

The classical asymmetrical bridge topology is employed as the driving circuit for the SRG under investigation and is shown in Fig. 4. The assumptions made are: 1) there is no saturation; 2) fringing effect is neglected around the pole corners; 3) mutual coupling among phases is neglected.

For the converter of Fig. 4, the voltage equation for each phase of the SRG is given [11] by

$$
\begin{aligned}
u_{ph} &= R_{ph}i_{ph} + \frac{d\lambda(i_{ph},\theta_r)}{dt} \\
&= R_{ph}i_{ph} + \frac{\partial\lambda(i_{ph},\theta_r)}{\partial i_{ph}}\frac{di_{ph}}{dt} + \omega_r\frac{\partial\lambda(i_{ph},\theta_r)}{\partial\theta_r} \\
&= R_{ph}i_{ph} + L_{ph}(\theta_r)\frac{di_{ph}}{dt} + \omega_r i_{ph}\frac{dL_{ph}}{d\theta_r}
\end{aligned}
\tag{5}
$$

where R_{ph} and i_{ph} are the phase resistance and phase current respectively, $\lambda(i_{ph},\theta_r)$ is the flux-linkage, ω_r is the rotor angular velocity and θ_r is the rotor position. The back emf e_{ph} is defined as

$$e_{ph} = \omega_r i_{ph}\frac{dL_{ph}}{d\theta_r} \tag{6}$$

and the incremental inductance $L_{ph}(\theta_r)$ is defined as

$$L_{ph}(\theta_r) = \frac{\partial\lambda(i_{ph},\theta_r)}{\partial i_{ph}} \tag{7}$$

If magnetic saturation is ignored, the instantaneous electro-magnetic torque is given [11] by:

$$T_e = \frac{1}{2}i_{ph}^2\frac{dL_{ph}}{d\theta_r} \tag{8}$$

where $dL_{ph}/d\theta_r$ is the slope of the phase inductance.

The main electrical losses of an SRG are copper losses and iron losses. Copper loss depends on the rms stator current [10] and is given by

$$P_{Cu} = mI_{rms}^2R_{ph} \qquad . \tag{9}$$

Iron loss is not uniformly distributed in the core owing to non-sinusoidal flux distribution and non-uniform flux harmonic spectra in various parts of the magnetic circuit. An approximate formulas based on Steinmetz equation could be used for iron loss calculation in an SRG [7]

$$P_{Fe} = c_h fB^{(a+bB)} + c_e\left(\frac{dB}{dt}\right)^2 \tag{10}$$

where f is the stroke frequency, c_h and c_e are the hysteresis and eddy-current loss coefficients, respectively, and a and b are coefficients that could be determined from the loss curves using a curve fitting procedure.

Since the amplitude of back emf varies with rotor speed, the behavior of the phase current depends on the relationship between back emf e_{ph} and source voltage u_0.

The typical waveforms of the idealized inductance, phase current, fluxlinkage of a current controlled SRG, for single-pulse operation are illustrated in Fig. 5 and Fig. 6 respectively. The operating stages of phase A are explained below with respect to Fig.5 and Fig.6.
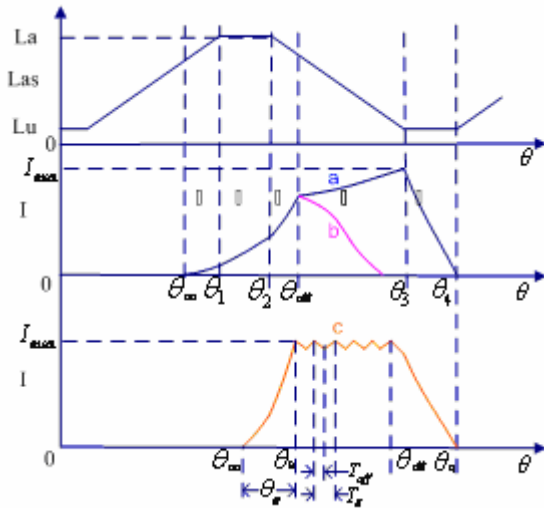
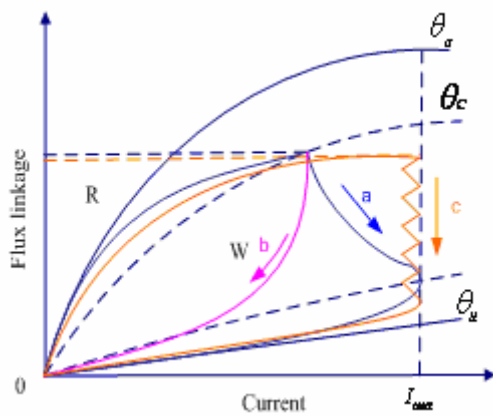Fig. 5: Inductance and typical phase current waveforms

Fig. 6: Typical flux linkage waveforms.

2. Operating modes

l) ($\theta_{on} \sim \theta_1$): exciting region; T1 and T2 are turned on to excite phase A. In this region, $u_{ph} = u_0$, $dL/d\theta > 0$, so $T_e > 0$; the back emf $e_{ph} < 0$, so the phase current increases slowly during this region. Part of the total power supplied is used for mechanical energy ($T_e > 0$) and the remaining is stored in the magnetic field. As a result, there will be slight drop in the generating efficiency during this mode. The duration of this mode is not constant and changes by a wide margin depending on the speed of the shaft, hence at higher speed the duration is shorter than that in lower speed. So, at high speed operation there is a need for storing energy in the field in advance to ensure the phase current reaches the rated value before the end of mode III.

) ($\theta_1 \sim \theta_2$): exciting region; T1 and T2 are still on; in this mode, the inductance reaches its maximum value at the aligned position and remains constant. So $u_{ph} = u_0$, $dL/d\theta = 0$, resulting in $T_e = 0$, as the back emf $e_{ph} = 0$ the phase current increases at a steeper rate. In this region, the input electrical energy is completely stored as field energy that will be used for the coming operating modes. The copper loss (9) can be minimized by proper regulation

of this mode so as to achieve a balance between the required field energy and the resulting copper loss.

III) ($\theta_2 \sim \theta_{off}$): exciting region; T1 and T2 are on; In this region the inductance decreases from its maximum value as the poles shift from the aligned position. It can be seen that $u_{ph} = u_0$, $dL/d\theta < 0$ resulting in $T_e < 0$, the back emf $e_{ph} > 0$, so the phase current sees a much steeper rate of increase compared to the previous mode. This stage is essential to establish enough phase current to store sufficient field energy by converting the electrical and mechanical energy into field energy.

) ($\theta_{off} \sim \theta_3$): generating region; T1 and T2 are OFF while D1 and D2 are ON; $u_{ph} = -u_0$, $dL/d\theta < 0$, so $T_e < 0$, the back emf $e_{ph} > 0$, and SRGs convert the mechanical energy into electrical energy. The phase current is now discharged into the load during this mode hence the name defluxing mode, and depending on the relative magnitude of back emf e_{ph} and source voltage u_0 , the phase current can have paths a or b as shown in fig.5 and fig. 6. During this mode, the mechanical energy and the field energy are converted into electrical energy.

a. Fig. 5 'a' curve corresponds to the condition when the back emf exceeds the dc link voltage as under high speed generating mode resulting in current rise beyond θ_{off} .

b. Fig. 5 'b' curve corresponds to the condition when the back emf is lower than the dc-link voltage resulting in the fall in phase current as under low speed generation.

) ($\theta_3 \sim \theta_4$): $u_{ph} = -u_0$, $dL/d\theta = 0$, so $T_e = 0$, the back emf $e_{ph} = 0$, and dc-link voltage causes phase current to fall to zero, the stored field energy is released and no mechanical energy(as $T_e = 0$) is converted into electrical energy in this mode.

3. Energy conversion loop analysis

Typical operating waveforms and the corresponding energy conversion loops for current controlled SRGs are shown in Fig. 5 and Fig. 6, respectively. We can define The energy ratio can be defined [11] as

$$Q = \frac{W}{S} = \frac{W}{W+R} \qquad (11)$$

where W , S , R are the converted energy, the supplied energy and the stored field energy respectively. The efficiency can be maximized by proper management of the phase current magnitude. It can be noted from (11) that the energy ratio is affected by any decrease in the converted energy W . For example, at low and medium speeds, the phase current falls after θ_{off} resulting in the net fall in the converted energy thus causing lower energy ratio Q. In order to improve Q, the phase current is modulated at a reference value as in fig. 5. Curve "c" using hysteresis control or PWM control in this region.

V. PROPOSED CONTROL SCHEME FOR THE SRWPG SYSTEM

The SRG can be controlled either in constant voltage mode [13] or constant power mode [8], [12]. In most cases the operation at constant power mode is preferred as maximum power can be obtained at any wind speed according to wind power curves in Fig. 3. In order to implement constant power control the current as well as the voltage must be sensed and multiplied and compared with the reference power signal. It is to be noted that the accuracy of the sampled instantaneous current signal is affected by the switching transients and sampling of current signal is difficult to be implemented. On the contrary, the voltage sampling does not suffer from the ripple problem faced by the current sampling because the voltage ripple can be reduced by increasing the dc-link capacitor and by increasing the filter capacitor at the hall-effect sampler.

Another advantage of this voltage mode control in this project is that the regulated voltage can be directly fed to a battery charge/discharge unit without the need for a separate dc-dc converter interface. The battery charge/discharge unit thus can be designed for a fixed input voltage. The battery charge/discharge unit can transfer the power from the generator whose output is a constant voltage to batteries which in turn will feed the power to other loads in the vehicle. Owing to the above reasons the voltage mode control was adopted for this project.
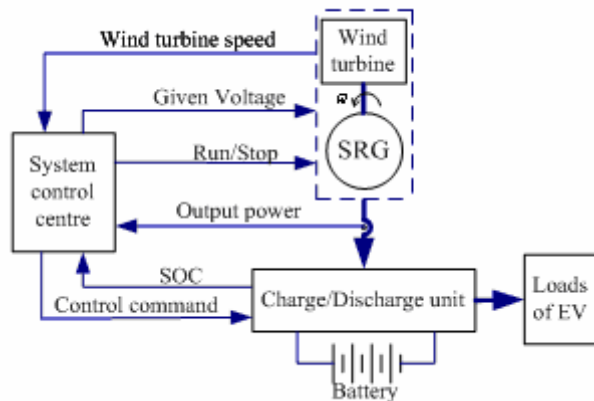

Fig. 7: The control schematic of the proposed SRWPG system

Increasing the generating efficiency and improving the battery charging mode are the two prime methods for optimizing this system. Fig. 7 shows the block diagram representation of the control scheme for the proposed system. A system control center is equipped with algorithms to ensure safe operation of the entire unit including generation and delivering power to the charge unit of the EV at high efficiency. On one hand, in order to increase the generating efficiency, the real time speed data is fed to the center in order to operate the turbine at its maximum power at different wind speeds (Fig. 3) by adjusting the given voltage or the control command for the charge/discharge unit. As the wind speed loop is the slower outer loop the implementation of real-time current sampling is not rigid for power control and hence is easy

to realize in practice. The control center will ensure that the turbine speed never falls out of the range between n_{min} and n_{max} (Fig. 3) for safety reason. On the other hand, in order to improve the safety of batteries during charging mode, the battery SOC is fed to the centre which regulates the command signal to the charge/discharge unit. Charging of the battery will be suspended if the SOC is out of the specified operating range of the battery.

VI. CONCLUSION

This paper has presented a novel EV: a wind power hybrid electric vehicle. A novel SRWPG system, as an important part of the novel EV, has been investigated in this work. The issues related to the structures and the fixed locations of the wind turbine for EVs are discussed, and a novel integrated wind turbine is proposed according to the requirements of the wind turbine for EVs. This paper has presented a novel control scheme for a SRWPG system according to the operating conditions and characteristic of the wind power and SRGs.

At present, there are a little research results in this direction. With the more stringent regulations on emissions and fuel economy, global warming, and constraints on energy resources, the wind power hybrid electric vehicle will attract more and more attention by automakers, governments, and customers in the future.

REFERENCES

[1] C. C. Chan, "The state of the art of electric, hybrid, and fuelcell vehicles," Proc. IEEE, vol. 95, no. 4, pp. 704-718, Apr. 2007.
[2] Ali Emadi, Heldon S Williamson, Alireza Khaligh, "Powerelectronics intensive solutions for advanced electric, hybrid electric, and fuel cell vehicular power systems", IEEE Trans. Power Electron., vol. 21, no. 3, pp. 567-577, May 2006.
[3] K. Rajashekara, J. Fattic, and H. Husted, "Comparative study of new on-board power generation technologies for automotive applications," in Proc. IEEE Workshop Power electron. transport., Auburn Hills, MI, Oct. 2002, pp. 3-10.
[4] B.R. Borchers and J.A. Locker, "Electrical system design of a solar electric vehicle," Electrical Insulation Conf., 1997 and Electrical Manufacturing & Coil Winding Conf., Sept. 1997, pp. 699 – 704.
[5] R. L. Maberry, "Wind Turbine Driven Generator System for a Motor Vehicle," United States Patent, Patent No. US 7,147,069 B2, Dec. 2006.
[6] K. W. Liskey, "Airflow Driven Electrical Generator for a Moving Vehicle," United States Patent, Patent No. US 6,857,492 B1, Feb. 2005.
[7] Y. Hayashi and T. J. E. Miller, "A new approach to calculate core losses in the SRM," IEEE. Trans. Ind. Appl., vol. 31, no. 5, pp. 1039-1046, Sep.-Oct. 1995.
[8] K. Ogawa, N. Yamamura, M. Ishda, "Study for Small Size Wind Power Generating System Using Switched Reluctance Generator," Industrial technology 2006 (ICIT 2006), IEEE International Conf., Dec. 2006, pp. 1510-1515.

[9] Y. C. Chang and C. M. Liaw, "On the Design of Power Circuit and Control Scheme for Switched Reluctance Generator," IEEE Trans. Power Electron., vol. 23, pp. 445-454, Jan. 2008.

[10] C. Mademlis and I. Kioskeridis, "Optimizing Performance in Current-Controlled Switched Reluctance Generators," IEEE Trans. Energy Conversion, vol. 20, pp. 556-565, Sept. 2005.

[11] T. J. E. Miller, Electronic Control of Switched Reluctance Machines. Oxford, U.K.: Newnes, 2001.

[12] R. Cardenas, R.Pena, M. Peraz, J. Clare, G. Asher, and P. Wheeler, "Control of a switched reluctance generator for variable-speed wind energy applications," IEEE trans. Energy Conversion, vol. 20, no. 4, pp. 781-791, Dec. 2005.

[13] A. Fleury, D. A. de Andrade, F. dos Santos e Silva and J. L. Domingos, "Switched reluctance generator for complementary wind power generation in grid connection," in IEMDC-IEEE, vol. 1, May 2007, pp. 465.